

Greatly enhanced intensity-difference squeezing via energy-level modulations in hot atomic media

Da Zhang^{1†}, Changbiao Li^{1†}, Zhaoyang Zhang¹, Yiqi Zhang¹, Yanpeng Zhang^{1*}, Min Xiao^{2,3*}

¹*Key Laboratory for Physical Electronics and Devices of the Ministry of Education & Shaanxi Key Lab of Information Photonic Technique, Xi'an Jiaotong University, Xi'an 710049, China*

²*Department of Physics, University of Arkansas, Fayetteville, Arkansas 72701, USA*

³*National Laboratory of Solid State Microstructures and School of Physics, Nanjing University, Nanjing 210093, China*

[†]Contributed equally to this work; ^{*} Corresponding author: ypzhang@mail.xjtu.edu.cn; mxiao@uark.edu

Narrow-band intensity-difference squeezing (IDS) beams have important applications in quantum metrology and quantum information. The best way to generate narrow-band IDS is to employ parametrically-amplified (PA) four-wave mixing (FWM) process in high-gain atomic media. Such IDS can be further enhanced by cascading multiple PA-FWM processes in separate atomic media. The complicated experimental setup, added losses and mechanical stability can limit the wide uses of such scheme in practical applications. Here, we show that by modulating/dressing the internal energy level(s) with additional laser(s), the degree of original IDS can be substantially increased. With an initial IDS of $-4.0\pm 0.1\text{dB}$ using PA-non-degenerate-FWM process in a three-level Λ -type configuration, the degree of IDS can be enhanced to $-7.0\pm 0.1\text{dB}/-8.1\pm 0.1\text{dB}$ when we use one/two laser beam(s) to modulate the involved ground/excited state(s). Our results show a low-loss, robust and efficient way to produce high degree of IDS and facilitate its potential applications.

Traditionally, quantum correlated bright laser beams are generated through parametrically-amplified (PA) optical down-conversion processes in nonlinear optical crystals^{1,2}. The produced entangled photons/beams typically have broad spectral width and therefore short coherence time due to the broad phase-matching width in nonlinear crystals³⁻⁵. Recently, narrow-band bright entangled light beams have been produced through PA four-wave mixing (PA-FWM) process in high-gain atomic media⁶. The intensity-difference squeezing (IDS) between the two beams can reach 5.0 dB⁷. Several interesting applications of using such narrow-band entangled beams, such as in entangled images⁸, FWM slow light⁹, delay of Einstein-Podolsky-Rosen entanglement^{10,11}, quantum metrology¹²⁻¹⁴, have all been experimentally demonstrated. In order to further increase the degree of IDS, the technique of cascading more stages of PA-FWM process has been employed. In one experiment, a second PA-FWM process in a separate atomic vapor cell was used to enhance the IDS from (-5.5 ± 0.1) dB/ (-4.5 ± 0.1) dB to (-7.0 ± 0.1) dB¹⁵. Similarly, enhanced continuous-variable squeezed states have also been realized by cascading two PA-down-conversion processes using two separate nonlinear crystals¹⁶. Ultimate enhancement limit reachable by using more stages of such cascade setups can be theoretically derived¹⁷. Although the cascading technique is conceptionally simple to consider, the added complications in the experimental setup and mechanical stability, as well as maintaining the phase coherence, between different stages will severely limit the broad applications in using such generated high degree of IDS.

Here we implement a totally different approach to enhance the IDS produced from the two correlated light beams generated from the PA-FWM process in a three-level Λ -type atomic system⁶. Since the degree of IDS is mainly determined by the high optical gain realizable in the PA-FWM process⁷, we set to find an efficient way to enhance the optical gain in the same atomic system. As previous studies shown, the optical gain can be significantly

increased by adding additional dressing fields to modulate the energy levels involved in the PA-FWM process¹⁸, which produces efficient higher-order multi-wave mixing processes¹⁹⁻²⁰. We first setup the standard measurement system for PA-FWM in a three-level Λ -type system in a heated rubidium vapor cell. An initial -4.0 dB IDS is obtained. Next, we drive the excited state with a laser beam connecting to an auxiliary energy level, which creates the dressed states and modifies the excited energy level in the original three-level system. Six-wave mixing (SWM) process comes into play in addition to the PA-FWM process^{18,21}, which significantly increases the gain in the system and therefore enhances the IDS to -7.0 dB. Finally, with another laser field simultaneously driving between one of the ground states and a second auxiliary energy level (i.e. double-dressing the original three-level system with two laser beams), a higher-order eight-wave mixing (EWM) process joins the co-existing PA-FWM and SWM ones^{19,20}, which further increases the system gain and, at the same time, enhances the IDS further to -8.1 dB.

This scheme of enhancing parametric gain, and therefore the generated IDS, in the system by modulating (dressing) the internal states of a multi-level atomic system has certain obvious advantages over using separate cascading stages in enhancing IDS. One is the simplicity in the experimental setup, since only one atomic medium is needed. The second is higher squeezing limit with less loss because of one stage rubidium cell. The third is mechanical stability by eliminating the need to maintain the relative vibrations and phase change between different stages. At the same time, the degree of IDS can not only be greatly enhanced, but also suppressed by simply varying the frequency detunings of the additional driving fields. These merits will greatly facilitate the potential applications of such IDS light sources in entanglement imaging⁸, quantum metrology¹²⁻¹⁴, quantum communications²²⁻²⁵ and quantum information processing^{22,25},

Results

Theoretical mode of energy-level modulation. Let us first consider the three-level Λ -type sub-system (involves levels $|0\rangle \leftrightarrow |2\rangle \leftrightarrow |1\rangle$), as shown in Fig. 1(b). A strong pump beam \mathbf{E}_1 (with frequency ω_1 , \mathbf{k}_1 , Rabi frequency G_1 , vertical polarization) is tuned to couple the D2 line transition and a weak beam \mathbf{E}_2 (ω_2 , \mathbf{k}_2 , G_2 , horizontal polarization) works as a probe field. The detuning $\Delta_i = \Omega_i - \omega_i$ is defined as the difference between the resonant transition frequency Ω_i and the laser frequency ω_i of \mathbf{E}_i . With the frequency of \mathbf{E}_1 tuned far away from the resonances, this system forms the standard PA-non-degenerate-FWM configuration to satisfy the phase-matching condition $\mathbf{k}_S^F + \mathbf{k}_{as}^F = 2\mathbf{k}_1$ (as shown in Fig. 1(c1)), and produces narrow-band IDS between the parametrically amplified probe (anti-Stokes) and conjugate (Stokes) beams⁶. The generated IDS mainly depends on the gain factor G_F in the anti-Stokes channel, i.e., the degree of IDS between \mathbf{E}_S and \mathbf{E}_{as} is given by⁶ $Sq_F = -\text{Log}_{10}(2G_F - 1)$. This nonlinear gain factor G_F can be modified by multiple parameters in multi-level coherent atomic systems.

Next, let us turn our attention to energy-level modulation (one-beam dressing) with an additional laser beam \mathbf{E}_3 (ω_3 , \mathbf{k}_3 , G_3 , Δ_3) in the ladder-type dressing scheme (Fig.1(b)). The interaction Hamiltonian of this \mathbf{E}_3 -dressed PA-FWM process can be expressed as (with all pump and dressing fields treated as classical fields):

$$H = \hbar \kappa_{F1}^{1d} \hat{a}^+ \hat{b}^+ \quad .H, \quad (1)$$

where \hat{a}^+ and \hat{b}^+ are the boson creation operators act on the electromagnetic excitation of the anti-Stokes and Stokes channel, $\kappa_{F1}^{1d} = |-i\varpi_{s/as} \chi_{F1}^{1d(3)} E_1^2 / 2|$ is the pumping parameter for the \mathbf{E}_3 -dressed PA-FWM process, which depends on the nonlinear susceptibility tensor $\chi_{F1}^{1d(3)}$ and the pump-field amplitude. $\varpi_{s/as}$ is the central frequency of generated Stokes or anti-Stokes signal. In the dressed-state picture, the third-order nonlinear susceptibility tensor

can be expressed as $\chi_{F1}^{1d(3)} = |N\mu_{20}\mu_{21}\rho_{F1(s/as)}^{1d(3)} / \varepsilon_0 \hbar E_1^2 G_{(s/as)}|$, where $\rho_{F1(s/as)}^{1d(3)}$ is the corresponding E_3 -dressed density-matrix element which can be obtained from Eqs. (S2)-(S3) in Supplemental Information (SI). Here, we define the E_3 -dressed nonlinear gain coefficient (related to the matrix element $\rho_{F1(s/as)}^{1d(3)}$) as $G_{F1}^{1d} = \cosh^2(\kappa_{F1}^{1d}L)$. The modified degree of IDS in this E_3 -dressed PA-FWM is given by

$$Sq_{F1}^{1d} = -\text{Log}_{10}(2G_{F1}^{1d} - 1). \quad (2)$$

This single-beam (E_3) modulated FWM process can be decomposed into co-existing FWM ($\mathbf{k}_S^F, \mathbf{k}_{aS}^F$) and SWM1 (with $\mathbf{k}_S^{S1} + \mathbf{k}_{aS}^{S1} = 2\mathbf{k}_1 + \mathbf{k}_3 - \mathbf{k}_3$, Fig. 1(c2)) processes^{20,21}. Therefore, κ_{F1}^{1d} , $\chi_{F1}^{1d(3)}$, and G_{F1}^{1d} are all greatly modified by the dressing field E_3 in Eqs. (S2)-(S3), (SI). With increased nonlinear gain factor G_{F1}^{1d} , Sq_{F1}^{1d} can be greatly enhanced. Similarly, we can obtain the one-beam E_4 ($\omega_4, \mathbf{k}_4, G_4, \Delta_4$) dressed PA-FWM gain factor G_{F2}^{1d} in the similar way and, therefore, achieve an enhanced IDS (Sq_{F2}^{1d}) in such V-type dressing configuration (Fig. 1(b)), which corresponds to co-existing the FWM and another SWM2 (with $\mathbf{k}_S^{S2} + \mathbf{k}_{aS}^{S2} = 2\mathbf{k}_1 + \mathbf{k}_4 - \mathbf{k}_4$) processes.

Finally, when the E_3 and E_4 beams turn on simultaneously (Fig.1(b)), a two-beam dressed PA-FWM configuration is formed, which generates co-existing FWM, SWM1, SWM2 and EWM (with $\mathbf{k}_S^E + \mathbf{k}_{aS}^E = 2\mathbf{k}_1 + \mathbf{k}_3 - \mathbf{k}_3 + \mathbf{k}_4 - \mathbf{k}_4$) processes (Fig. 1(c3)). We can obtain the two-beam-modulated gain factor G_F^{2d} and IDS Sq_F^{2d} in this five-level atomic system. The expression for the modulated third-order nonlinearity (Eqs. (S2)-(S3), SI) clearly reveals why the gains of the modified (dressed) PA-FWM systems can be greater than the original PA-FWM process, and therefore the enhanced IDS.

Note that we have used different orders of multi-wave mixing (MWM) processes to describe the modified (dressed) PA-FWM processes, which give a clear physical picture for

the complicated situations and is valid under certain approximations on the dressing fields^{26,27}.

With the clear decompositions of the dressed-state formalism for the multi-beam-dressed PA-FWM, we can better identify the contributions of the enhanced/modified IDS from different wave-mixing processes. Such methods show a robust and efficient way to produce high degree of IDS.

Enhanced IDS with one dressing field (either E_3 or E_4). There are two ways to dress the Λ -type three-level ($|0\rangle \leftrightarrow |2\rangle \leftrightarrow |1\rangle$) system, one by applying E_3 between levels $|2\rangle$ and $|3\rangle$ (i.e., ladder-dressing configuration) and another by applying E_4 between levels $|0\rangle$ and $|4\rangle$ (V-dressing configuration), as shown in Fig. 1(b), which modify the original PA-FWM process differently, and therefore provide different enhancement factors for IDS. In the following, we consider their effects separately.

Figure 2 shows PA-FWM signals in the probe and corresponding conjugate channels in the three-level Λ -type ^{85}Rb atomic system, respectively, with and without the E_3 beam. With E_3 off and the pump field detuning Δ_1 detuned to ~ 1.12 GHz, we scan the probe field E_2 over 8 GHz across D2 line and observe a number of features in transmission and its conjugate channels, as shown in Figs. 2(a1) and 2(a3), respectively. When E_3 turns on, as shown in Fig. 1(c2), the one-beam dressing FWM (coexisting FWM+SWM)²⁰ signal in Fig. 2(a2) gets stronger than that in Fig. 2(a1), which indicates an enhanced FWM process. The E_3 -dressed PA-FWM signal is enhanced due to the constructive interference between FWM and SWM1(\mathbf{k}_s^{s1} , \mathbf{k}_{as}^{s1}), satisfying the dressed enhancement condition $\Delta_1 + \Delta_3 \pm \sqrt{\Delta_3^2 + 4|G_3|^2} / 2 = 0$. Similar to the probe channel, the corresponding conjugate signal is also enhanced due to the existing PA-SWM1 process, as shown in Fig. 2(a4). So, the dressed gain coefficient G_{F1}^{ld} is enhanced compared to the gain coefficient G_F without the E_3 beam (Fig. 2(a3)).

The measured IDS of the PA-FWM signal (Fig. 2(b2)) is -3.6 ± 0.1 dB below the

normalized SQL. With the dressing field E_3 on, the measured IDS of the E_3 -dressed FWM signal (Fig. 2(b3)) is about -6.1 ± 0.1 dB below the SQL, which indicates that the degree of IDS (Sq_{F1}^{1d} in Eq. (2)) is significantly increased by the enhanced nonlinear gain coefficient G_{F1}^{1d} due to the E_3 dressing effect, as shown in Fig. 2(b3). Furthermore, one can infer IDS of the pure PA-SWM1 to be -2.8 ± 0.1 dB.

Actually, the IDS can not only be enhanced, it can also be suppressed under certain condition. Figures 2(c1) and 2(c3) show the features of PA-FWM signal in a three-level Λ -type system. With the dressing field E_3 turned on and detuned to about -1.15 GHz, the intensities of the dressed FWM signals in both probe and conjugate channels (Figs. 2(c2) & 2(c4), respectively) are suppressed as compared to the PA-FWM signals in Figs. 2(c1) and 2(c3). Since the two-photon resonant condition $\Delta_1 + \Delta_3 = 0$ is satisfied, there exists a destructive interference between the generated FWM and SWM1 fields^{26,27}. This results in a decreased dressed gain G_{F1}^{1d} . The IDS (Sq_{F1}^{1d}) of E_3 -dressed FWM signals is measured to be -2.1 ± 0.1 dB (Fig. 2(d3)), which is smaller than that of the original PA-FWM (-4.0 ± 0.1 dB as in Fig. 2(d2)). Therefore, the parametric gain and degree of IDS in the original PA-FWM system can be fully modulated (either enhanced or suppressed) by the additional field E_3 .

Next, we consider the case with E_4 -dressed PA-FWM instead of E_3 . Figures 3(a2) and 3(c2) show that, compared to the original PA-FWM (Figs. 3(a1) & 3(c1)), the E_4 -dressed FWM signal in the probe channel can be either enhanced or suppressed. The field E_4 dresses the ground state $|0\rangle$ and creates the dressed states $|G_{4\pm}\rangle$. Thus, due to the fulfillments of dressed enhancement and suppression conditions, i.e., $\Delta_1 - \Delta_4 \pm \sqrt{\Delta_4^2 + 4|G_4|^2} / 2 = 0$ and $\Delta_1 - \Delta_4 = 0$, the PA-FWM signal can be either enhanced or suppressed¹⁸⁻²⁰. The increase or decrease of the probe and conjugate field (\mathbf{k}_{aS}^{s2} , \mathbf{k}_S^{s2}) intensities (Figs. 3(a2) & (c2)) is caused by constructive or destructive interference between the generated FWM and SWM2 fields.

Therefore, the corresponding dressed gain $G_{F_2}^{1d}$ becomes large or small accordingly.

Figures 3(b) and 3(d) depict the measured IDS of E_4 -dressed FWM, corresponding to enhanced (Fig. 3(b)) and suppressed (Fig. 3(d)) conditions, respectively. The measured degree of IDS ($Sq_{F'}^{1d}$) for this E_4 -dressed FWM (Fig. 3(b3)) is -7.0 ± 0.1 dB, which is much larger than that of the original PA-FWM (-3.6 ± 0.1 dB) (Fig. 3(b2)). Moreover, the inferred -3.7 ± 0.1 dB IDS for the PA-SWM2 process is larger than the -2.8 dB IDS for the PA-SWM1 process with E_3 dressing shown in Fig. 2(b3). The reason is that E_4 has effects of both population transfer and dressing ($G_{F'}^{1d} = G^P + G_{F_2}^{1d}$, Section 3 in SI) while E_3 only has the dressing gain ($G_{F_1}^{1d}$), resulting in a much larger total nonlinear gain $G_{F'}^{1d}$ for the E_4 -dressed case.

However, due to the existed population gain G^P for the V-type dressing scheme, the E_4 -dressed PA-FWM cannot realize a suppression of IDS below the original PA-FWM value. In fact, under the suppressed gain condition (destructive interference between the FWM and SWM2 fields), the measured IDS of the E_4 -dressed PA-FWM is still as large as -6.5 ± 0.1 dB (Fig. 3(d3)).

Enhanced IDS with two dressing fields. Finally, let's consider the case with both E_3 and E_4 dressing fields on at the same time for the five-level system, as shown in Fig. 1(b), with phase-matching conditions given in Fig. 1(c3). Figures 4(a) and 4(b) show modified PA-FWM signals in the probe and conjugate channels, respectively, when different beam(s) are blocked. As the frequency detunings of E_3 and E_4 set to be -0.9 GHz and 0.95 GHz, the intensity of dressed PA-FWM is expected to increase relative to Fig. 4(a1), as shown in Figs. 4(a2) and 4(a3), respectively. Similar to Figs. 2(a2) and 3(a2), two newly generated PA-SWM signals, i.e., SWM1 and SWM2, increase in Fig. 4(a2) and (a3). Particularly, with E_3 and E_4 both on simultaneously, a two-beam-dressed FWM signal in Fig. 4(a4) is greatly enhanced, which is the mixture of one pure PA-FWM, two SWM and one EWM processes. At the same time, the

intensity of the two-beam-dressed conjugate signal (E_S) is also changed accordingly, as shown in Fig. 4(b). So, the two-beam dressing gain G_F^{2d} is significantly enhanced.

Figure 4(c) presents the measured degrees of IDS for modified PA-FWM signals in Figs. 4(a) and 4(b). First, with all external dressing fields (E_3 & E_4) blocked, and the IDS of pure PA-FWM is measured to be -3.6 ± 0.1 dB (Fig. 4(c2)). The curve (c1) gives the SQL. When either E_3 or E_4 is on, the measured IDS of one-beam-dressed FWM is 5.0 ± 0.1 dB (Fig. 4(c3)) or 6.1 ± 0.1 dB (Fig. 4(c4)), respectively. When both dressing fields (E_3 and E_4) are on at the same time, the measured IDS of two-beam-dressed FWM (Fig. 4(c5)) reaches -8.1 ± 0.1 dB. This largely increased degree of IDS is caused by the enhancement in two-beam-dressed PA-FWM gain with coexisting and constructive interfered PA-FWM, SWM and EWM processes in the system. The inferred degree of IDS for the pure PA-EWM is -2.3 ± 0.1 dB (Sq_F^{2d} in Eq. (S10), SI). Moreover, the total degree of IDS can be easily controlled and modulated by adjusting the frequency detunings of the dressing fields.

Conclusions

We have observed the greatly enhanced IDS for one- and two-beam modulated PA-FWM processes in the same hot atomic system. Compared to the simple PA-FWM case (with -4.0 dB IDS), the degrees of IDS for E_3 - and E_4 -modulated PA-FWM processes are measured to be -6.1 dB and -7.0 dB, respectively. The IDS for the two-beam-dressed PA-FWM process gets to be -8.1 dB, which indicates that the generated higher-order PA-MWM processes contribute to the total parametric gain and therefore the quantum noise suppression (or enhanced IDS). Under different dressing frequency detunings, the generated high-order nonlinear signals can interfere either constructively, which enhances the total parametric gain, or destructively, which reduces the total gain. Since the parametric gain is directly related to the degree of generated IDS for the probe and conjugate beams, the obtained degree of IDS can be fully controlled. Compared to the previously demonstrated methods of using separate cascading

stages in enhancing IDS¹⁵, the current scheme of modulating (dressing) the internal states of a multi-level atomic system has several obvious advantages. One is its simplicity in the experimental setup, since only one atomic medium is needed and less optical elements will be used. The second is higher squeezing limit with less loss because of one stage rubidium cell. The third is the mechanical stability by eliminating the needs to maintain the relative vibrations and phase changes between different cascading stages. At the same time, the degree of IDS can not only be greatly enhanced, but also suppressed by simply varying the frequency detunings of the added driving fields. Our current experiment demonstrates a robust and efficient way to produce high degree of IDS on an integrated platform which can find potential applications in quantum metrology and quantum information processing.

Methods

Experimental setup. The five relevant energy levels are $5S_{1/2}, F=2$ ($|0\rangle$), $5S_{1/2}, F=3$ ($|1\rangle$), $5P_{3/2}$ ($|2\rangle$), $5D_{5/2}$ ($|3\rangle$), $5P_{1/2}$ ($|4\rangle$) in ^{85}Rb , as shown in Fig. 1(b). Levels $|0\rangle \leftrightarrow |2\rangle \leftrightarrow |1\rangle$ form the basic Λ -type three-level system. We use light of 500 mW from a CW Ti:Sapphire laser as the 780 nm pump beam (E_1), and another light up to 0.2 mW from an external cavity diode laser as the 780 nm probe beam (E_2). They couple with the Λ -type atomic system in a naturally abundant rubidium vapor cell by a polarizing beam splitter (PBS). The vapor cell is wrapped with μ -metal sheets to shield stray magnetic field from environment and heated to 125°C to provide an atomic density of $3 \times 10^{13} \text{cm}^{-3}$. E_2 propagates in the same direction as E_1 with a small angle of 0.26° . These two laser beams form the standard double- Λ configuration and produce the PA-FWM IDS. When E_4 (795 nm, 4 mW) is added onto E_1 (in the same direction) and E_3 (776 nm, 8 mW) counter-propagates with E_1 , they establish two electromagnetically induced transparency (EIT) windows in the system and significantly modify (dressing) the

original PA-FWM process^{21,28}. The spatial alignments of the beams are shown in Fig. 1(a). The output probe and conjugate beams are detected by two balanced photodetectors and the difference of the two detected signals is sent to a radio frequency (RF) spectrum analyzer to display the noise power in a fixed bandwidth as a function of frequency. All noise measurements in this paper are taken at an analysis frequency of 1 MHz.

The noise spectra of the relative intensities between the probe and conjugate channels are measured next. First, E_1 passes through an acousto-optic modulator (AOM) of 1.5 GHz twice to have a frequency difference of 3 GHz. The beam is then injected into the probe channel and the field E_2 is off. In order to calibrate the standard quantum limit (SQL) for the total optical power arriving at the photodetectors, a coherent beam with the same power is split by a 50/50 beam splitter. The two beams are directed into the balanced photodetectors and the noise power of the intensity difference is measured. All noise power spectra are normalized to the corresponding SQL shown in Fig. 2(b1). As the SQL is dependent on the signal intensity, we need to normalize the SQL of PA-FWM according to that of E_3 -dressed FWM signals. In Fig. 2(a2), since E_3 -dressed FWM signal is enhanced as compared to the PA-FWM (Fig. 2(a1)), the SQL of PA-FWM is moved upward by 1.2 dB relative to that of E_3 -dressed FWM (Fig. 2(b1)). However, due to the suppression of PA-FWM in Fig. 2(c2), the SQL of PA-FWM is moved downward by 0.45 dB to the curve in Fig. 2(d1). Thus, the SQL in the enhanced case is higher than the SQL in the suppressed case.

References

- [1] Wu L A, Kimble H J, Hall J L, et al. Generation of squeezed states by parametric down conversion. *Phys. Rev. Lett.* **57**, 2520 (1986).
- [2] Kwiat P G, Mattle K, Weinfurter H, et al. New high-intensity source of polarization-entangled photon pairs. *Phys. Rev. Lett.* **75**, 4337 (1995).
- [3] Hübel H, Hamel D R, Fedrizzi A, et al. Direct generation of photon triplets using cascaded photon-pair

- sources. *Nature* **466**, 601-603 (2010).
- [4] Shalm L K, Hamel D R, Yan Z, et al. Three-photon energy-time entanglement. *Nat. Phys.* **9**, 19-22 (2013).
- [5] Lemos G B, Borish V, Cole G D, et al. Quantum imaging with undetected photons. *Nature* **512**, 409-412 (2014).
- [6] McCormick C F, Boyer V, Arimondo E, et al. Strong relative intensity squeezing by four-wave mixing in rubidium vapor. *Opt. Lett.* **32**, 178-180 (2007).
- [7] Zhou N, Kinzel E C, Xu X. Complementary bowtie aperture for localizing and enhancing optical magnetic field. *Opt. Lett.* **36**, 2764-2766 (2011)
- [8] Boyer V, Marino A M, Pooser R C, et al. Entangled images from four-wave mixing. *Science* **321**, 544-547 (2008).
- [9] Camacho R M, Vudiyasetu P K, Howell J C. Four-wave-mixing stopped light in hot atomic rubidium vapour. *Nat. Photon.* **3**, 103-106 (2009).
- [10] Marino A M, Pooser R C, Boyer V, et al. Tunable delay of einstein–podolsky–rosen entanglement. *Nature* **457**, 859-862 (2009).
- [11] Clark J B, Glasser R T, Glorieux Q, et al. Quantum mutual information of an entangled state propagating through a fast-light medium. *Nat. Photon.* **8**, 515-519 (2014).
- [12] Giovannetti V, Lloyd S, Maccone L. Quantum metrology. *Phys. Rev. Lett.* **96**, 010401 (2006).
- [13] Napolitano M, Koschorreck M, Dubost B, et al. Interaction-based quantum metrology showing scaling beyond the Heisenberg limit. *Nature* **471**, 486-489 (2011).
- [14] Hudelist F, Kong J, Liu C, et al. Quantum metrology with parametric amplifier-based photon correlation interferometers. *Nat. Commun.* **5**, 3049 (2014).
- [15] Qin Z, Cao L, Wang H, et al. Experimental generation of multiple quantum correlated beams from hot rubidium vapor. *Phys. Rev. Lett.* **113**, 023602 (2014).
- [16] Jia X, Yan Z, Duan Z, et al. Experimental realization of three-color entanglement at optical fiber communication and atomic storage wavelengths. *Phys. Rev. Lett.* **109**, 253604 (2012).
- [17] Wang D, Zhang Y, Xiao M. Quantum limits for cascaded optical parametric amplifiers. *Phys. Rev. A* **87**, 023834 (2013).
- [18] Zheng H, Zhang X, Zhang Z, et al. Parametric amplification and cascaded-nonlinearity processes in

- common atomic system. *Sci. Rep.* **3**, 1885 (2013).
- [19] Zhang Y, Brown A W, Xiao M. Opening four-wave mixing and six-wave mixing channels via dual electromagnetically induced transparency windows. *Phys. Rev. Lett.* **99**, 123603 (2007).
- [20] Zhang Y, Khadka U, Anderson B, et al. Temporal and spatial interference between four-wave mixing and six-wave mixing channels. *Phys. Rev. Lett.* **102**, 013601 (2009).
- [21] Kang H, Hernandez G, Zhu Y. Slow-light six-wave mixing at low light intensities. *Phys. Rev. Lett.* **93**, 073601 (2004).
- [22] Lvovsky A I, Raymer M G. Continuous-variable optical quantum-state tomography. *Rev. Mod. Phys.* **81**, 299-332 (2009).
- [23] Einstein A, Podolsky B, Rosen N. Can quantum-mechanical description of physical reality be considered complete?. *Phys. Rev.* **47**, 777 (1935).
- [24] Davidovich L. Sub-Poissonian processes in quantum optics. *Rev. Mod. Phys.* **68**, 127-173 (1996).
- [25] Weedbrook C, Pirandola S, García-Patrón R, et al. Gaussian quantum information. *Rev. Mod. Phys.* **84**, 621 (2012).
- [26] Zhang Y, Xiao M. Generalized dressed and doubly-dressed multi-wave mixing. *Opt. Express* **15**, 7182-7189 (2007).
- [27] Zuo Z, Sun J, Liu X, et al. Generalized n-photon resonant 2n-wave mixing in an (n+1)-level system with phase-conjugate geometry. *Phys. Rev. Lett.* **97**, 193904 (2006).
- [28] Wu Y, Saldana J, Zhu Y. Large enhancement of four-wave mixing by suppression of photon absorption from electromagnetically induced transparency. *Phys. Rev. A* **67**, 013811 (2003)

Acknowledgements

M.X. and Y.P.Z acknowledge partial support from NBRPC (2012CB921804). Y.P.Z was also supported by KSTIT of Shaanxi Province (2014KCT-10) and NSFC (11474228).

Author contributions

Y.P.Z. and M.X. planned the project. D.Z., C.B.L. and Z.Y.Z. carried out the experiment; D.Z. and Y.Q.Z. provided the theoretical supports. Y.P.Z. supervised the research project. D.Z., C.B.L., Y.P.Z. and M.X. wrote the manuscript with inputs from all authors.

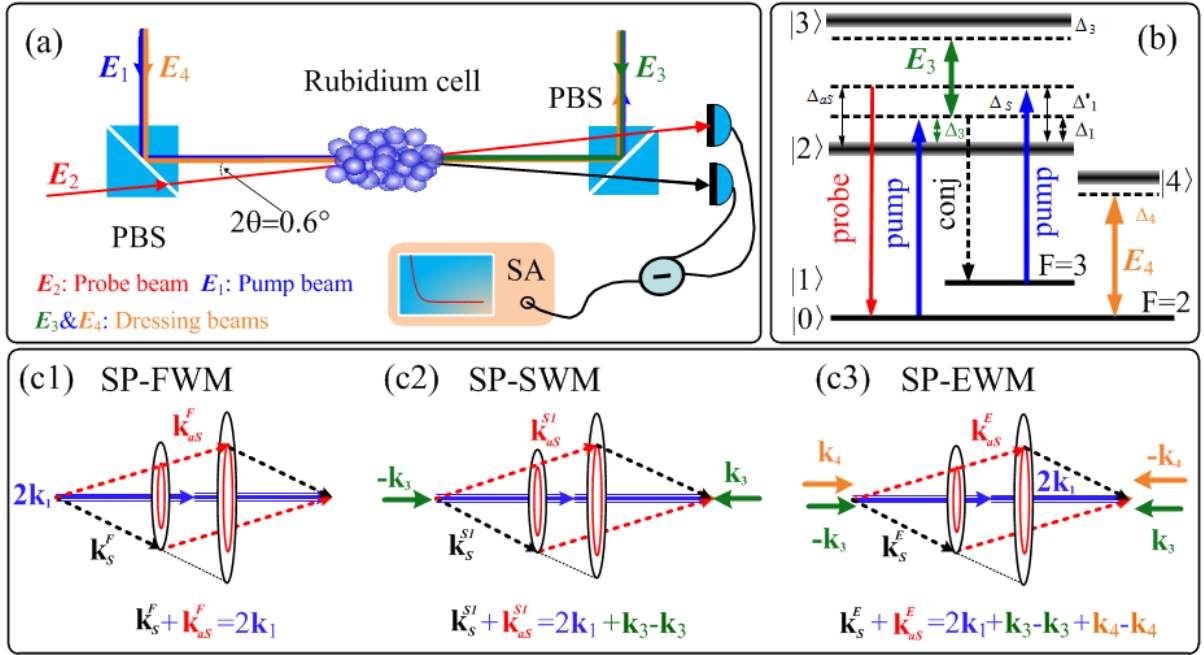


Figure 1 | (a) **Experimental setup.** PBS: polarizing beam splitter; SA: spectrum analyzer. (b) Energy level diagram of the Λ -type ($|0\rangle \leftrightarrow |2\rangle \leftrightarrow |1\rangle$) rubidium atomic system with an E_3 ladder-type dressing (between levels $|2\rangle$ and $|3\rangle$) and an E_4 V-type dressing (between levels $|0\rangle$ and $|4\rangle$) simultaneously. (c1)-(c3) Phase-matching conditions for the spontaneous parametric FWM (SP-FWM), SP-SWM1 and SP-EWM processes, respectively.

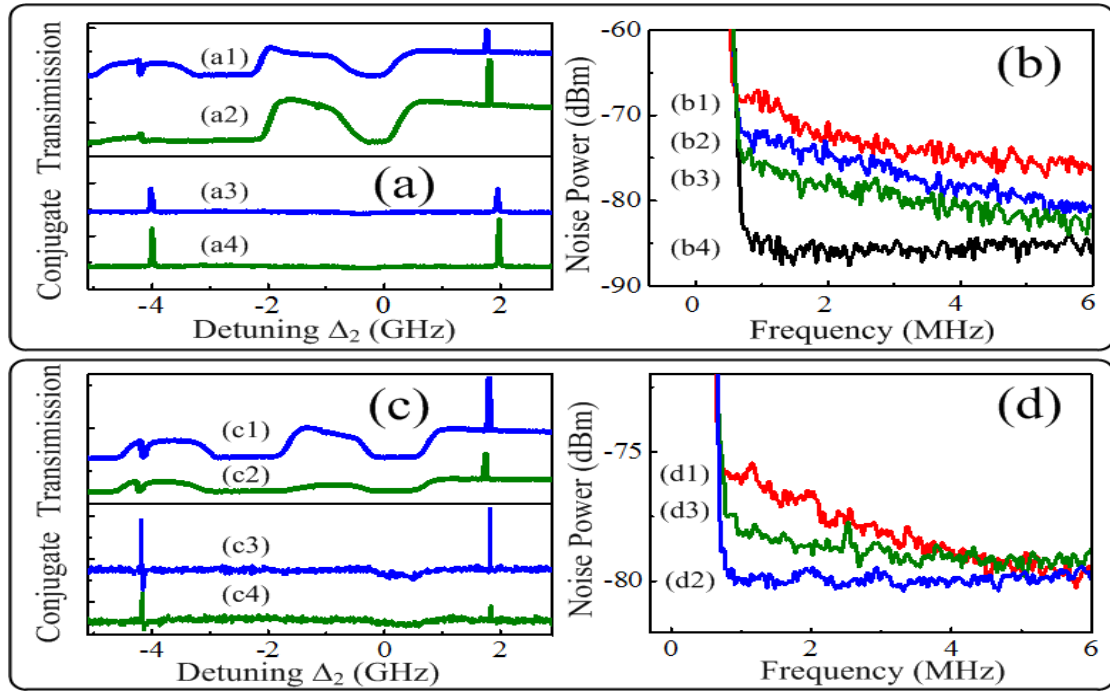


Figure 2 | Measured noise spectra and modulated IDS with E_3 -beam dressing. (a) Measured probe transmission signal (E_{as}) and corresponding conjugate signal (E_s) versus probe frequency detuning. (a1) & (a3) are with E_3 off and (a2) & (a4) E_3 on, and $\Delta_1 = 1.12$ GHz, $\Delta_3 = -1$ GHz. (b) Relative intensity noise levels versus spectrum analyzer frequency. (b1)-(b4) SQL, FWM, dressed FWM (FWM+SWM1) when E_3 is applied, and electronic noise, respectively. (c) & (d) All experimental conditions are the same as in (a) and (b) except $\Delta_1 = 1.15$ GHz and $\Delta_3 = -1.15$ GHz.

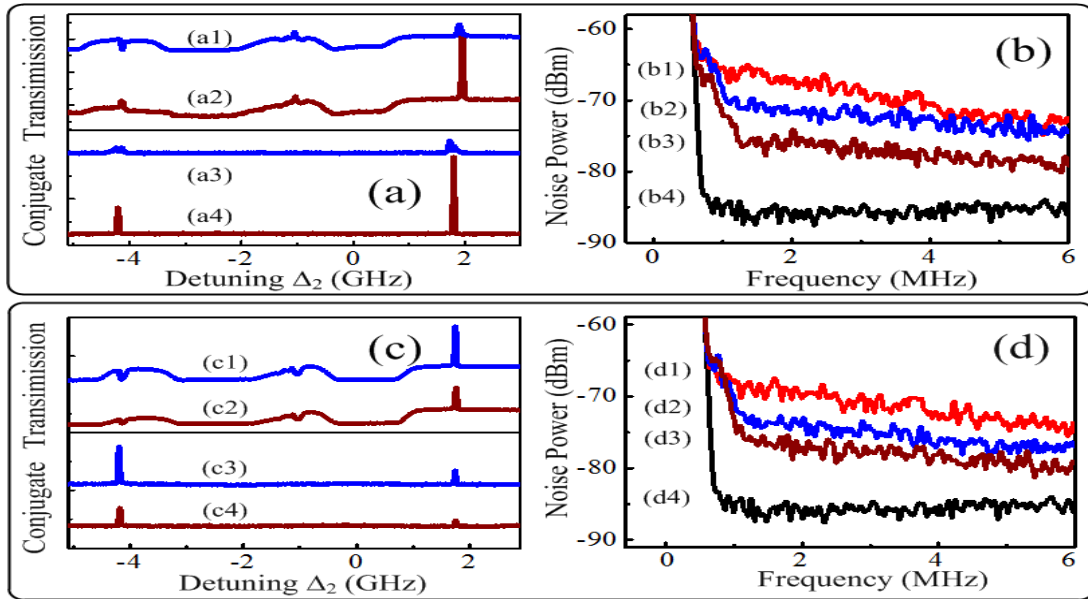


Figure 3 | Measured noise spectra and modulated IDS with E_4 -beam dressing. (a1) & (a3) are with E_4 off. (a2) & (a4) with E_4 on, and $\Delta_1=1.12$ GHz, $\Delta_4=-1$ GHz. (b1)-(b4) SQL, FWM, dressed FWM (FWM+SWM2) when field E_4 is applied, and electronic noise, respectively. (c) & (d) $\Delta_1=1.15$ GHz, $\Delta_4=1.15$ GHz, respectively.

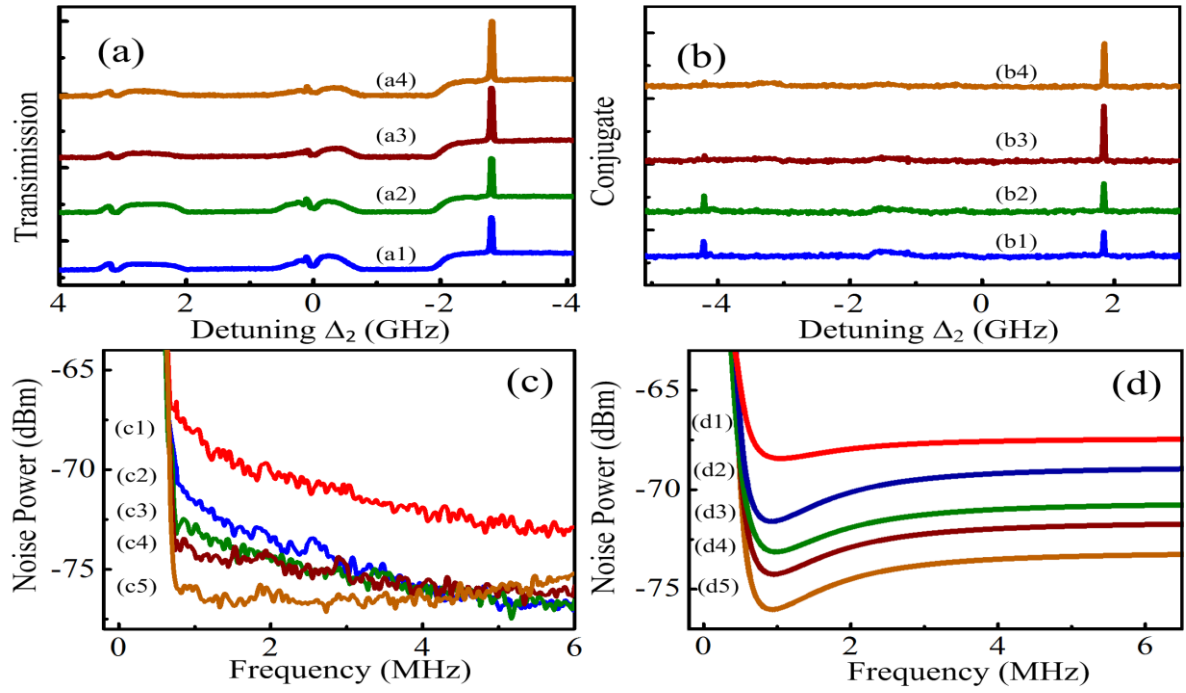


Figure 4 | Measured noise spectra and enhanced IDS with both E_3 and E_4 beams on simultaneously.

(a) Measured probe transmission signal (E_{as}) versus the probe detuning. (a1) E_3 and E_4 off; (a2) E_3 on; (a3) E_4 on; (a4) E_3 and E_4 both on, and set $\Delta_1=1.12$ GHz, $\Delta_3=-0.9$ GHz and $\Delta_4=0.95$ GHz. (b1)-(b4) corresponding conjugate signal (E_s) of (a1)-(a4), respectively. (c) Relative intensity noise spectra versus spectrum analyzer frequency. (c1)-(c5) SQL, FWM, E_3 -dressed FWM, E_4 -dressed FWM, and E_3 - & E_4 -dressed FWM (FWM+SWM+EWM), respectively. (d) Theoretical simulation of squeezing curve, correspond to (c1)-(c5).